

Controlling the self-doping of $\text{YBa}_2\text{Cu}_3\text{O}_{7-\delta}$ polar surfaces: From Fermi surface to nodal Fermi arcs by ARPES

M.A. Hossain,¹ J.D.F. Mottershead,¹ A. Bostwick,² J.L. McChesney,² E. Rotenberg,²
R. Liang,³ W.N. Hardy,^{1,3} G.A. Sawatzky,^{1,3} I.S. Elfimov,³ D.A. Bonn,^{1,3} and A. Damascelli^{1,3,*}

¹*Department of Physics & Astronomy, University of British Columbia, Vancouver, British Columbia V6T 1Z1, Canada*

²*Advanced Light Source, Lawrence Berkeley National Laboratory, Berkeley, California 94720, USA*

³*AMPEL, University of British Columbia, Vancouver, British Columbia V6T 1Z4, Canada*

The discovery of quantum oscillations in the normal-state electrical resistivity of $\text{YBa}_2\text{Cu}_3\text{O}_{6.5}$ [1] provides the first evidence for the existence of Fermi surface (FS) pockets in an underdoped cuprate. However, the pockets' electron vs. hole character, and the very interpretation in terms of closed FS contours, are the subject of considerable debate [2, 3, 4, 5, 6, 7, 8, 9, 10, 11, 12, 13, 14]. Angle-resolved photoemission spectroscopy (ARPES), with its ability to probe electronic dispersion as well as the FS, is ideally suited to address this issue. Unfortunately, the ARPES study of $\text{YBa}_2\text{Cu}_3\text{O}_{7-\delta}$ (YBCO) has been hampered by the technique's surface sensitivity [15, 16, 17]. Here we show that this stems from the polarity and corresponding self-doping of the YBCO surface. By in-situ deposition of potassium atoms on the cleaved surface, we are able to continuously tune the doping of a single sample from the heavily overdoped to the underdoped regime. This reveals the progressive collapse of the normal-metal-like FS into four disconnected nodal FS arcs, or perhaps into hole but not electron pockets, in underdoped YBCO6.5.

The key to the high- T_c cuprate puzzle is understanding the evolution of the low-energy normal-state electronic structure, upon doping charge carriers into the CuO_2 planes, from the underdoped antiferromagnetic charge-transfer insulator to the overdoped normal metal. This sets the stage for the emergence of high- T_c superconductivity at intermediate doping. A spectacular account of this remarkable evolution has been provided by the collapse - upon underdoping - of the normal-state FS. In the heavily overdoped regime, angular magnetoresistance oscillation [18] and ARPES experiments [19, 20] on $\text{Tl}_2\text{Ba}_2\text{CuO}_{6+\delta}$ have arrived at a very precise quantitative agreement in observing a coherent band-structure-like FS. Upon reducing the number of holes in the CuO_2 planes, however, the hole FS volume decreases consistently with Luttinger's theorem until below optimal doping, at which point the single-particle FS appears to reduce to four disconnected nodal Fermi arcs [21, 22, 23]. This scenario was suggested from ARPES studies of Bicu-prates [21, 22] and $\text{Ca}_{2-x}\text{Na}_x\text{CuO}_2\text{Cl}_2$ [23], and is naturally connected to the existence of the pseudogap.

The detection of quantum oscillations in oxygen-

ordered ortho-II YBCO6.5 calls the Fermi arc scenario into question, suggesting instead a FS reconstruction into either hole and/or electron pockets [1, 5, 6]. Due to the complex multiband and correlated character of the electronic structure of YBCO6.5 [7], the determination of the nature of these pockets and their generality to the underdoped cuprates requires connecting transport and single-particle spectroscopy information on the same underdoped system. The study of YBCO6.5 by ARPES is thus of extremely high priority. Unfortunately, this material is complicated by the presence of CuO -chain layers and the lack of a neutral [001] cleavage plane (Fig. 1a). More specifically, YBCO cleaves between the CuO chain layer and the BaO layer, leaving on the cleaved surface relatively large regions ($>100 \text{ \AA}$) of either CuO or BaO terminations. Scanning-tunneling microscopy shows that the CuO chain terraces are characterized by prominent surface density waves [24] and differ substantially from the bulk: as also seen in ARPES [15], they exhibit surface states and unavoidable doping disorder. Recent ARPES studies of nearly optimally doped YBCO indicated that CuO and BaO terminations give different contributions to the total photoemission intensity [17], with a doping $p = 0.3$ for the top-most CuO_2 planes

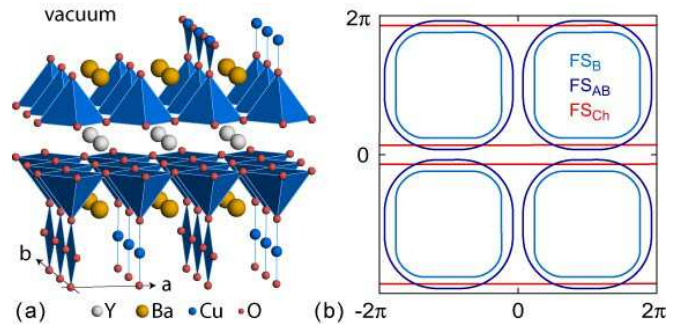


FIG. 1: **The surface of cleaved YBCO.** (a) Structure of oxygen-ordered YBCO6.5 (with alternating oxygen full and empty chains), showing the BaO and CuO chain terminations of the cleaved surface. Electronic reconstruction takes place at these polar surfaces, similar to the prototypical case of a polar catastrophe in ionic insulators with a $|1+|1-|1+|1-|\dots$ layer-by-layer charge [27, 28]. This leads to ‘overdoped-like’ FS features for the surface topmost layers, as shown pictorially in (b) for CuO_2 -plane bonding and antibonding bands (FS_B and FS_{AB}), and the one-dimensional CuO chain band (FS_{Ch}).

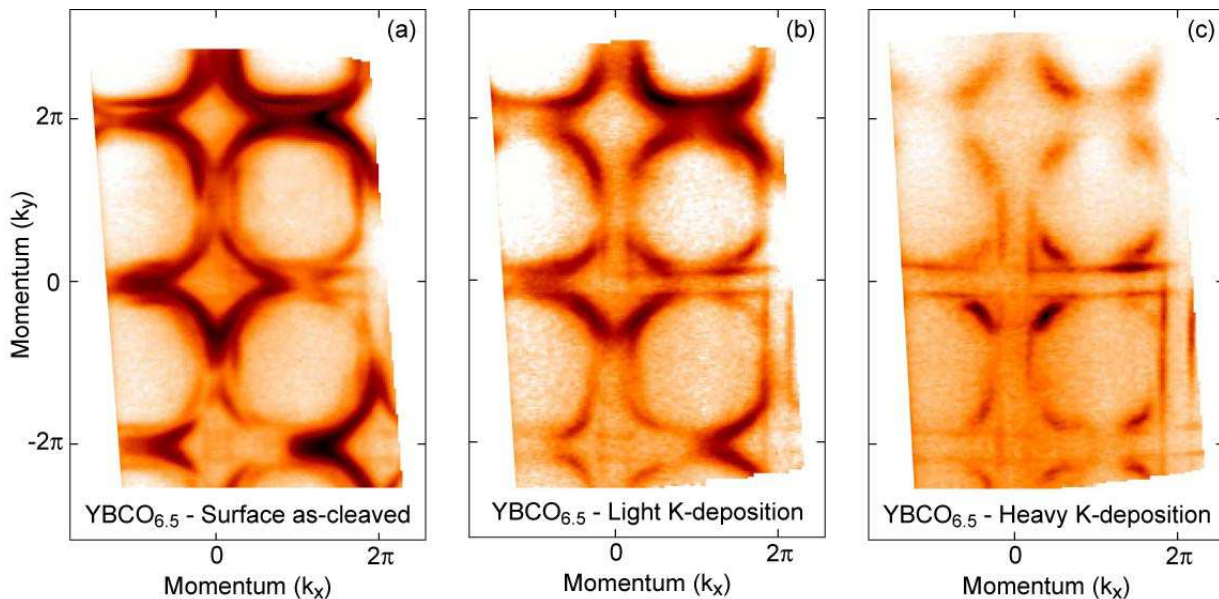


FIG. 2: **YBCO FS evolution upon e^- doping.** (a) ARPES FS of as-cleaved YBCO6.5, exhibiting an effective hole doping $p = 0.28$ per planar Cu atom, as determined from the average area of bonding and antibonding CuO_2 -bilayer FSs. (b,c) By evaporating potassium on the same sample (< 1 monolayer), electrons are transferred to the top-most CuO_2 bilayer and the corresponding FSs become progressively more hole-underdoped. (c) For heavy K-deposition ($p = 0.11$ as estimated from the area of the chain FS), the E_F ARPES intensity reduces to the 1D CuO chain FS and four disconnected nodal CuO_2 FS arcs.

almost irrespective of the nominal bulk doping. This corresponds to heavy overdoping all the way into the non-superconducting regime (Fig. 4), and is actually not achievable in bulk, fully-oxygenated YBCO7.0 for which $p = 0.194$ [25]. Similar problems have been encountered in the ARPES study of $\text{YBa}_2\text{Cu}_4\text{O}_8$ [26].

Overcoming these problems requires, first of all, recognizing that the cleaved surface of YBCO is actually polar. This can lead to overdoped-like FSs (Fig. 1b) even as a result of a pure electronic reconstruction [27, 28]. A wide momentum distribution map of the FS from ‘as-cleaved’ YBCO6.5 is presented in Fig. 2a (Methods). The ARPES data are a superposition of features from the BaO and CuO terminated regions: because of the few Å probing depth at these photon energies, the ARPES intensity from the BaO -terminated regions is dominated by the CuO_2 -bilayer bands and that from the CuO -terminated regions by the chain band. The comparison with Fig. 1b, allows one to identify the FS features originating from the CuO_2 -plane bonding and antibonding bands (FS_B and FS_{AB}), and the one-dimensional (1D) CuO chain band (FS_{Ch}). Note that the strong momentum-dependent intensity modulation of the ARPES features, which seems inconsistent with the sample symmetry, is simply a manifestation of the matrix elements effects associated with the photon/crystal/electron geometry changing across the field of view (no symmetrization was performed). Also, this particular ortho-II sample happened to be twinned, in the bulk and not just on the surface, as confirmed by x-ray diffraction (this has an effect on FS_{Ch} but

not on the discussion of the four-fold symmetric Fermi arcs). Most importantly, the fit of the two-dimensional ARPES FSs over multiple zones returns the following areas, counting electrons, relative to the Brillouin zone area $A_{BZ} = 4\pi^2/ab$: the bonding Fermi surface $\text{FS}_B = 46.2\%$, the antibonding $\text{FS}_{AB} = 26.0\%$, and the chain surface $\text{FS}_{Ch} = 13.8\%$. From the average of bonding and antibonding FS areas, one can calculate the hole-doping $p = 0.28 \pm 0.01$ per planar copper ($p = 0$ for the $1/2$ -filled Mott insulator with 1 hole per Cu atom). As summarized in the phase diagram of Fig. 4, this indicates that the self-doping of the YBCO6.5 polar surface is that of a non-superconducting, heavily-overdoped cuprate.

The next step is that of actively controlling the self-doping of the surface, so as to reduce its hole content down to the value of underdoped, bulk YBCO6.5. This can be achieved by evaporating potassium in situ on the cleaved surface (Methods): owing to the low ionization potential, K^{1+} ions are adsorbed on the surface and electrons are doped into the top-most layers. As a consequence, we would anticipate the evolution of all detected features towards the underdoped regime of hole-doped cuprates, which is precisely what one can observe in Fig. 2, upon increasing the K^{1+} concentration (i.e., decreasing the hole doping) from panel a to c. The doping is indeed changing according to an increase in electron filling (all data were acquired on the same sample after subsequent K evaporations). This is evidenced by the continuous FS_{Ch} area increase (counting electrons), which evolves from $\text{FS}_{Ch} = 13.8\%$ for the as-cleaved surface to

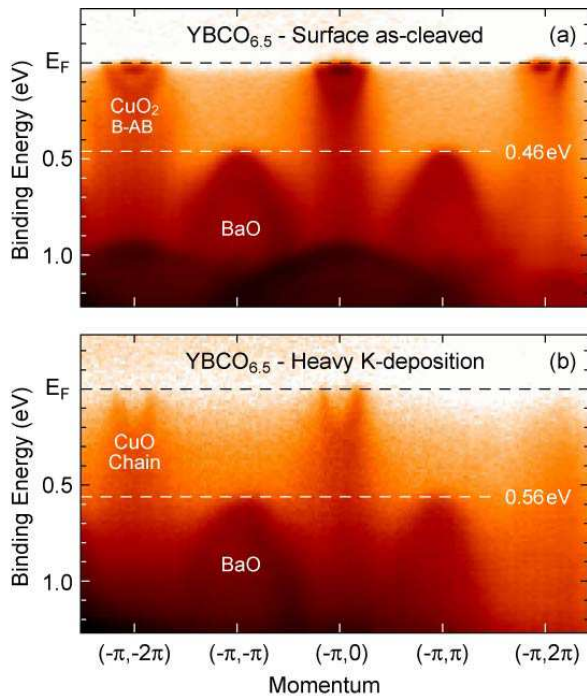


FIG. 3: **YBCO band evolution upon e^- doping.** (a) Electronic band dispersion as revealed by the E -vs.- k ARPES intensity map for as-cleaved YBCO6.5. (b) Upon K deposition, electrons are added as evidenced by the high binding energy shift of the BaO bands; at the same time, the intensity of bonding (B) and antibonding (AB) CuO₂ features vanishes and only the CuO chain band is detected at the antinodes.

$FS_{Ch}^{K1} = 14.7\%$ and $FS_{Ch}^{K2} = 16.6\%$ for the increasingly K-deposited YBCOK1 (Fig. 2b) and YBCOK2 (Fig. 2c). By comparing the carrier concentration per chain-Cu measured by the FS_{Ch} area with the results of ab-initio LDA band structure calculations [7], we can estimate the corresponding hole-doping per planar-Cu. This way we find good agreement with the value $p=0.28$ already estimated for as-cleaved YBCO6.5 from the average of FS_B and FS_{AB} . Most importantly, however, we obtain a hole-doping $p^{K1} = 0.20$ and $p^{K2} = 0.11$ for YBCOK1 and YBCOK2, which means that the surface of YBCOK2 is very close to the doping level $p=0.097$ of bulk YBCO6.5.

The most interesting aspect of the data in Fig. 2 is the evolution of the CuO₂-plane features. For heavy K deposition (Fig. 2c), the LDA-like CuO₂-bilayer bonding and antibonding FSs of overdoped YBCO have collapsed into four nodal Fermi arcs, consistent with other underdoped cuprates [21, 22, 23]. This is accompanied by the complete suppression of CuO₂ antinodal spectral intensity as well as nodal bilayer splitting, which were instead clearly resolved for as-cleaved YBCO6.5 (Fig. 2a). Their disappearance with K deposition hints at a severe loss of coherence upon underdoping. Correspondingly the CuO₂ nodal Fermi wavevectors, relative to the Brillouin zone diagonal $(0, 0)-(\pi, \pi)$, have evolved from $k_F^{AB} = 0.29$ and

$k_F^B = 0.36$ for ‘overdoped’ as-cleaved YBCO6.5, to a single $k_F^{K2} = 0.40$ for ‘underdoped’ YBCOK2. These numbers compare well to what has been observed on other cuprates at similar dopings (note that the following are both single CuO₂-layer systems): $k_F = 0.36$ and 0.41 , respectively, for overdoped $p = 0.26$ Tl₂Ba₂CuO_{6+ δ} [19] and underdoped $p = 0.12$ Ca_{2-x}Na_xCuO₂Cl₂ [23].

The transfer of electrons to the surface of YBCO upon K deposition is also confirmed by an inspection of the electronic dispersions along the $(-\pi, -2\pi)-(-\pi, 2\pi)$ direction in momentum space. On as-cleaved YBCO6.5 (Fig. 3a), we detect well-defined bonding and antibonding CuO₂ bands crossing E_F at the antinodes, as well as the BaO band with a maximum binding energy at the zone corners $(-\pi, \pm\pi)$. On YBCOK2 (Fig. 3b), the BaO band is now located ~ 100 meV deeper in energy. This indicates a shift of the chemical potential consistent with the transfer of electrons from adsorbed K atoms to the top-most BaO, CuO-chain, and CuO₂-plane layers. At the same time, on underdoped $p = 0.11$ YBCOK2 the only coherent feature detected at the antinodes is the 1D CuO chain band; the antinodal CuO₂-plane spectral weight has now become fully incoherent.

We would now like to summarize our findings, illustrated by the phase diagram and symmetrized FS data for YBCOK2 and as-cleaved YBCO6.5 in Fig. 4. Our study demonstrates that the self-hole-doping of the cleaved polar surfaces of YBCO can be controlled by the in-situ evaporation of alkali metals, in the present case K. This novel approach paves the way for the study of this important material family – across the whole phase diagram – by single particle spectroscopies. As this material has been the gold standard in a number of seminal bulk-sensitive studies of the normal and superconducting properties, the direct connection with single-particle spectroscopy can lead to an understandable underdoped anchor point, analogous to Tl₂Ba₂CuO_{6+ δ} in the overdoped regime [20]. The results obtained for $p = 0.11$ YBCOK2 establish that the ARPES FS of underdoped YBCO consists of the superposition of 1D CuO chain FS and CuO₂-plane-derived nodal Fermi arcs. It is thus consistent, with the additional complication of the chains, to what has already been observed in oxychloride [23] and Bi-cuprates [21, 22]. In this sense, the disruption of the large hole-like coherent FS in underdoped cuprates is a truly universal phenomenon.

Having obtained the first momentum resolved FS data for underdoped YBCO, it becomes crucial to understand the connection between ARPES and quantum oscillation results [1, 6]. First, the detection of the BaO band maximum at ~ 0.5 eV below E_F does not validate the scenario coming from LDA band structure calculations, which suggested that the small Fermi surface found in the quantum oscillation measurements might originate from small pockets produced by BaO-Cu_{chain} bands at $(\pm\pi, \pm\pi)$ [7, 8]. We also did not observe any signature of CuO₂-

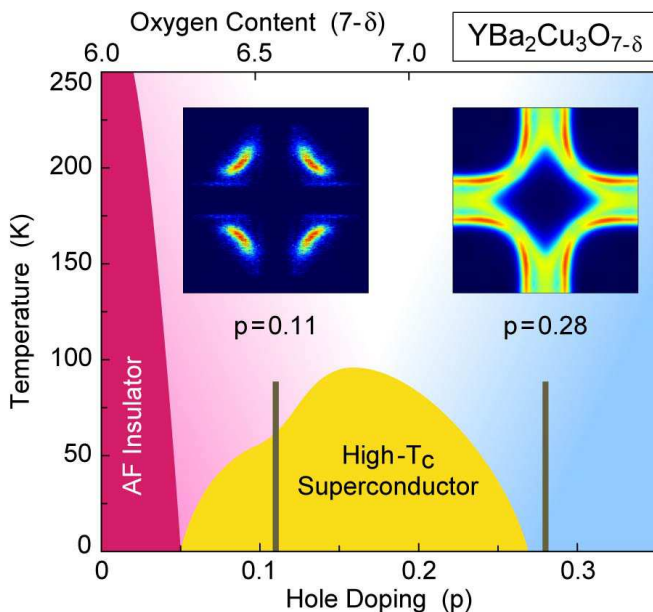


FIG. 4: **Phase diagram of YBCO by ARPES.** Schematic temperature-doping phase diagram of YBCO adapted from Ref. 1. The hole doping p per planar copper ($p = 0$ for the $1/2$ -filled Mott insulator with 1 hole per Cu atom), and the corresponding oxygen content ($7-\delta$), are indicated on bottom and top horizontal axes respectively [25]. The ARPES FS for under- and overdoped YBCO is also shown; the momentum-distribution maps have been 2-fold and 4-fold symmetrized for $p = 0.11$ and 0.28 , respectively. Similar to the data in Fig. 2, the doping levels were determined for $p = 0.11$ from the area of FS_{Ch} , and for $p = 0.28$ from the area of FS_B and FS_{AB} .

derived band folding arising from the ortho-II oxygen-ordering of the chains [7, 8], which is possibly consistent with the loss of three-dimensional coherence evidenced by the suppression of bilayer band splitting upon underdoping. Recent measurements of the Hall resistance in high magnetic field have noted a sign change with decreasing temperature [5], suggesting that the quantum oscillations seen on top of a negative Hall coefficient might come from small electron pockets, rather than the hole pockets originally proposed [1]. However, there is no sign of such electron pockets in our ARPES data from underdoped YBCO K2, nor are there signs of additional zone-folding due to the kinds of density wave instabilities that might give rise to such a Fermi surface reconstruction [4, 5, 11].

If any pocket had to be postulated on the basis of the present ARPES data, the most obvious possibility would be that the Fermi arcs are in fact hole-like nodal Fermi pockets, as obtained for light doping of the antiferromagnetic parent compound in self-consistent Born calculations [29] and already speculated from the study of other underdoped cuprates [21, 22, 23]. The lack of a finite ARPES intensity on the outer side of the pockets would be consistent with the strong drop in the quasiparticle coherence $Z_{\mathbf{k}}$ expected beyond the antiferromagnetic zone

boundary [9, 30]. To estimate an area for these ostensible nodal pockets, we can fold the detected arc profile, either with respect to the antiferromagnetic zone boundary or the end points of the arc itself, obtaining values of either 2.6% or 1.3%, relative to the full Brillouin zone area $A_{BZ} = 4\pi^2/ab$. These numbers compare relatively well with the pocket area 1.9% suggested on the basis of quantum oscillation experiments on bulk YBCO6.5 [1, 6]. However, these are hole, not electron pockets.

At present, this seems to be a crucial disagreement between the interpretations of a single-particle spectroscopy and bulk transport measurements on underdoped YBCO. The interpretation of the Hall resistance is likely to be complicated, since it necessarily invokes multiple bands with different scattering and can also be influenced by strong correlations, the presence of localized magnetic moments, and also the vortex liquid. It should also be noted that these transport measurements are made in high magnetic field whereas the ARPES data are acquired in zero field. Nevertheless, there appears to be a discrepancy which must be resolved, especially since the YBCO ARPES data presented here are consistent with the large body of single particle spectroscopy information obtained on other cuprates [21, 22, 23].

Whatever the solution to the puzzle outlined above, it should be emphasized that the present approach, based on the in-situ alkaline metal evaporation on freshly cleaved surfaces, opens the door to this type of manipulation of other cuprates and complex oxides, not only to control the self-doping of polar surfaces but also to reach doping levels otherwise precluded in the bulk. For instance, one could try to underdope the surface of $Tl_2Ba_2CuO_{6+\delta}$, which grows naturally overdoped [20], or even to obtain an electron-doped superconductor starting from the insulating parent compounds.

METHODS

Sample preparation. YBa₂Cu₃O_{6+x} single crystals were grown in non-reactive BaZrO₃ crucibles using a self-flux technique. The CuO_x chain oxygen content was set to $x = 0.51$ by annealing in a flowing O₂:N₂ mixture and homogenized by further annealing in a sealed quartz ampoule, together with ceramic at the same oxygen content. After mounting for the cleave required in an ARPES measurement, the samples were cooled from 100 °C to room temperature over several days to establish the ortho-II superstructure ordering of the CuO_x chain layer [32]. The particular sample used in the present study was twinned, as confirmed by x-ray diffraction after the ARPES measurements.

ARPES experiments. ARPES measurements [31] were carried out on the Electronic Structure Factory endstation at Beamline 7.01 of the Advanced Light

Source (ALS). The data were measured with linearly-polarized 110 eV photons and a Scienta R4000 electron analyzer in angle-resolved mode. YBCO6.5 single crystals were cleaved in situ at a base pressure better than 2.5×10^{-11} torr and then oriented by taking fast Fermi surface scans. Several procedures were tried out on these samples in an attempt to suppress the surface contribution to the total photoemission intensity and gain direct insight into the bulk electronic structure. For instance, samples were temperature-cycled between 20 and 100 K [33], or were cleaved at higher temperature (~ 80 K) and then cooled down to 20 K [34], in order to age and/or vary the characteristics of the cleaved surfaces. While both procedures have proved successful in measuring the bulk dispersion and FS of layered Sr_2RuO_4 [33, 34], no effect was observed in the case of YBCO6.5. Successful control of the self-doping of the cleaved surfaces was achieved by in-situ deposition of submonolayers of potassium, with a commercial SAES getter source [35], on freshly cleaved YBCO6.5. In this latter case, the samples were kept at 20 K at all times during the cleaving, K-deposition, and ARPES measurements. All ARPES data shown in Fig. 2, 3, and 4 were obtained on the same sample, i.e. as-cleaved and after two subsequent K evaporations. Energy and angular resolutions were set to ~ 30 meV and 0.2° ($\pm 15^\circ$ angular window) for the data in Fig. 2 and 3, and to ~ 30 meV and 0.1° ($\pm 7^\circ$ angular window) for the higher-quality FS mappings in Fig. 4.

* Electronic address: damascelli@physics.ubc.ca

- [1] Doiron-Leyraud, N. *et al.* Quantum oscillations and the Fermi surface in an underdoped high- T_c superconductor. *Nature* **447**, 565-568 (2007).
- [2] Yelland, E. A. *et al.* Quantum oscillations in the underdoped cuprate $\text{YBa}_2\text{Cu}_4\text{O}_8$. Preprint at <http://arxiv.org/abs/0707.0057> (2007).
- [3] Bangura, A. F. *et al.* Shubnikov-de Haas oscillations in $\text{YBa}_2\text{Cu}_4\text{O}_8$. Preprint at <http://arxiv.org/abs/0707.4461> (2007).
- [4] Balakirev, F. F. *et al.* Fermi surface reconstruction at optimum doping in high- T_c superconductors. Preprint at <http://arxiv.org/abs/0710.4612> (2007).
- [5] LeBoeuf, D. *et al.* Electron pockets in the Fermi surface of hole-doped high- T_c superconductors. *Nature* **450**, 533-536 (2007).
- [6] Jaudet, C. *et al.* de Haas-van Alphen oscillations in the underdoped cuprate $\text{YBa}_2\text{Cu}_3\text{O}_{6.5}$. Preprint at <http://arxiv.org/abs/0711.3559> (2007).
- [7] Elfimov, I. S., Sawatzky, G. A. & Damascelli, A. Fermi pockets and correlation effects in underdoped $\text{YBa}_2\text{Cu}_3\text{O}_{6.5}$. Preprint at <http://arxiv.org/abs/0706.4276> (2007).
- [8] Carrington, A. & Yelland, E. A. Band-structure calculations of Fermi-surface pockets in ortho-II $\text{YBa}_2\text{Cu}_3\text{O}_{6.5}$. *Phys. Rev. B* **76**, 140508 (2007).
- [9] Harrison, N., McDonald, R. D. & Singleton, J. Cuprate Fermi orbits and Fermi arcs: the effect of short-range antiferromagnetic order. *Phys. Rev. Lett.* **99**, 206406 (2007).
- [10] Chen, W.-Q., Yang, K.-Y., Rice, T. M. & Zhang, F. C. Quantum oscillations in magnetic field induced antiferromagnetic phase of underdoped cuprates: application to ortho-II $\text{YBa}_2\text{Cu}_3\text{O}_{6.5}$. Preprint at <http://arxiv.org/abs/0706.3556> (2007).
- [11] Millis, A. J. & Norman, M. Antiphase stripe order as the origin of electron pockets observed in 1/8-hole-doped cuprates. Preprint at <http://arxiv.org/abs/0709.0106> (2007).
- [12] Chakravarty, S. & Kee, H.-Y. Fermi pockets and quantum oscillations of the Hall coefficient in high temperature superconductors. Preprint at <http://arxiv.org/abs/0710.0608> (2007).
- [13] Alexandrov, A. S. Theory of quantum magneto-oscillations in underdoped cuprate superconductors. Preprint at <http://arxiv.org/abs/0711.0093> (2007).
- [14] Melikyan, A., Vafeek, O. Quantum oscillations in the mixed state of d -wave superconductor. Preprint at <http://arxiv.org/abs/0711.0776> (2007).
- [15] Schabel, M. C. *et al.* Angle-resolved photoemission on untwinned $\text{YBa}_2\text{Cu}_3\text{O}_{6.95}$. I. Electronic structure and dispersion relations of surface and bulk bands. *Phys. Rev. B* **57**, 6090 (1998).
- [16] Lu, D. H. *et al.* Superconducting gap and strong in-plane anisotropy in untwinned $\text{YBa}_2\text{Cu}_3\text{O}_{7-d}$. *Phys. Rev. Lett.* **86**, 4370 (2001).
- [17] Zabolotnyy, V. B. *et al.* Momentum and temperature dependence of renormalization effects in the high-temperature superconductor $\text{YBa}_2\text{Cu}_3\text{O}_{7-d}$. *Phys. Rev. B* **76**, 064519 (2007).
- [18] Hussey, N.E. , Abdel-Jawad, M., Carrington, A., Mackenzie, A.P. & Ballcas, L. A coherent three-dimensional Fermi surface in a high-transition-temperature superconductor. *Nature* **425**, 814-817 (2003).
- [19] Platé, M. *et al.* Fermi surface and quasiparticle excitations of overdoped $\text{Tl}_2\text{Ba}_2\text{CuO}_{6+\delta}$ by ARPES. *Phys. Rev. Lett.* **95**, 077001 (2005).
- [20] Peets, D. C. *et al.* $\text{Tl}_2\text{Ba}_2\text{CuO}_{6+\delta}$ brings spectroscopic probes deep into the overdoped regime of the high- T_c cuprates. *New Journ. Physics* **9**, 1-32 (2007).
- [21] Norman, M. R. *et al.* Destruction of the Fermi surface in underdoped high- T_c superconductors. *Nature* **392**, 157-160 (1998).
- [22] Kanigel, A. *et al.* Evolution of the pseudogap from Fermi arcs to the nodal liquid. *Nature Physics* **2**, 447-451 (2006).
- [23] Shen, K. M. *et al.* Nodal quasiparticles and antinodal charge ordering in $\text{Ca}_{2-x}\text{Na}_x\text{CuO}_2\text{Cl}_2$. *Science* **307**, 901-904 (2005).
- [24] Derro, D. J. *et al.* Nanoscale one-dimensional scattering resonances in the CuO chains of $\text{YBa}_2\text{Cu}_3\text{O}_{6+x}$. *Phys. Rev. Lett.* **88**, 097002 (2002).
- [25] Liang, R., Bonn, D. A. & Hardy, W. N. Evaluation of CuO_2 plane hole doping in $\text{YBa}_2\text{Cu}_3\text{O}_{6+x}$ single crystals. *Phys. Rev. B* **73**, 180505 (2006).
- [26] Kondo, T. *et al.* Dual character of the electronic structure of $\text{YBa}_2\text{Cu}_4\text{O}_8$: the conduction bands of CuO_2 planes and CuO chains. *Phys. Rev. Lett.* **98**, 157002 (2007).
- [27] Hesper, R., Tjeng, L. H., Heeres, A. & Sawatzky, G. A. Photoemission evidence of electronic stabilization of

- polar surfaces in K_3C_{60} . *Phys. Rev. B* **62**, 16046-16055 (2000).
- [28] Nakagawa, N., Hwang, H.Y. & Muller, D.A. Why some interfaces cannot be sharp. *Nature Materials* **5**, 204-209 (2006).
- [29] Sushkov, O. P., Sawatzky, G. A., Eder, R. & Eskes, H. Hole photoproduction in insulating copper oxide. *Phys. Rev. B* **56**, 11769-11776 (1997).
- [30] Eskes, H. & Eder, R. Hubbard model versus t-J model: the one-particle spectrum. *Phys. Rev. B* **54**, 14226-14229 (1996).
- [31] Damascelli, A. Probing the electronic structure of complex systems by state-of-the-art ARPES. *Phys. Scripta* **T109**, 61-74 (2004); (<http://arxiv.org/abs/0307085>) (2003).
- [32] Liang, R., Bonn, D. A. & Hardy, W. N. Preparation and x-ray characterization of highly ordered ortho-II phase $YBa_2Cu_3O_{6.50}$ single crystals. *Physica C* **336**, 57-62 (2000).
- [33] Damascelli, A. *et al.* Fermi surface of Sr_2RuO_4 from angle resolved photoemission. *J. Electron Spectr. Relat. Phenom.* **114-116**, 641-646 (2001).
- [34] Damascelli, A. *et al.* Fermi surface, surface states, and surface reconstruction in Sr_2RuO_4 . *Phys. Rev. Lett.* **85**, 5194-5197 (2000).
- [35] Ohta, T., Bostwick, A., Seyller, T., Horn, K. & Rotenberg, E. Controlling the electronic structure of bilayer graphene. *Science* **313**, 951-954 (2006).

ACKNOWLEDGMENTS

This work was supported by the Alfred P. Sloan Foundation (A.D.), an ALS Doctoral Fellowship (M.A.H.), the CRC Program (A.D. and G.A.S), NSERC, CFI, CIFAR Quantum Materials, and BCSI. The Advanced Light Source is supported by the Director, Office of Science, Office of Basic Energy Sciences, of the U.S. Department of Energy under Contract No. DE-AC02-05CH11231.

AUTHORS INFORMATION

Correspondence and requests for materials should be addressed to A. Damascelli (damascelli@physics.ubc.ca).